10-26-2018

Metabolic reprogramming of murine cardiomyocytes during autophagy requires the extracellular nutrient sensor decorin.

Maria A. Gubbiotti
Thomas Jefferson University

Erin L. Seifert
Thomas Jefferson University

Ulrich Rodeck
Thomas Jefferson University

Jan B. Hoek
Thomas Jefferson University

Renato V. Iozzo
Thomas Jefferson University

Metabolic reprogramming of murine cardiomyocytes during autophagy requires the extracellular nutrient sensor decorin

Received for publication, June 21, 2018, and in revised form, July 19, 2018 Published, Papers in Press, July 26, 2018, DOI 10.1074/jbc.RA118.004563

Maria A. Gubbiotti[‡], Erin Seifert[‡§], Ulrich Rodeck[‡¶], Jan B. Hoek[‡§], and Renato V. Iozzo[‡1]

From the [‡]Department of Pathology, Anatomy and Cell Biology and the Cancer Cell Biology and Signaling Program, Sidney Kimmel Medical College, Thomas Jefferson University, Philadelphia, Pennsylvania 19107, [§]MitoCare Center, Department of Pathology, Anatomy and Cell Biology, Thomas Jefferson University, Philadelphia, Pennsylvania 19107, and [¶]Department of Dermatology and Cutaneous Biology, Thomas Jefferson University, Philadelphia, Pennsylvania 19107

Edited by George N. DeMartino

The extracellular matrix is a master regulator of tissue homeostasis in health and disease. Here we examined how the small, leucine-rich, extracellular matrix proteoglycan decorin regulates cardiomyocyte metabolism during fasting *in vivo*. First, we validated in $Dcn^{-/-}$ mice that decorin plays an essential role in autophagy induced by fasting. High-throughput metabolomics analyses of cardiac tissue in $Dcn^{-/-}$ mice subjected to fasting revealed striking differences in the hexosamine biosynthetic pathway resulting in aberrant cardiac *O*-β-*N*-acetylglycosylation as compared with WT mice. Functionally, $Dcn^{-/-}$ mice maintained cardiac function at a level comparable with non-fasted animals whereas fasted WT mice showed reduced ejection fraction. Collectively, our results suggest that reduced sensing of nutrient deprivation in the absence of decorin preempts functional adjustments of cardiac output associated with metabolic reprogramming.

Decorin, a small, leucine-rich proteoglycan localized to the extracellular matrix (1–3), regulates numerous functions to maintain cellular homeostasis as well as to prevent tumorigenesis (4, 5), making it a *bona fide* "guardian from the matrix" (6). Most recently, the research surrounding decorin has involved studying its increasingly important role in the control of catabolism. Specifically, decorin initiates autophagy in endothelial (7, 8) and glioma cells (9) and mitophagy in triple-negative breast carcinoma cells (10) via its interaction with and signaling through receptor tyrosine kinases (RTKs)[2]. Furthermore, decorin is itself an autophagy-sensitive factor (11) where it is induced in response to nutrient deprivation as well as following direct mTOR inhibition. Additionally, we discovered that mice lacking decorin are insensitive to starvation-induced cardiac autophagy following a 1-day period of fasting (11).

In the context of metabolism and metabolic disorders, nutrient and energy status are emerging as intimate partners with autophagy and its deregulation. In particular, research in this area illustrates that abnormal glucose metabolism results in augmented flux through the hexosamine biosynthetic pathway (HBP), leading to increased levels of protein *O*-GlcNAcylation and consequent inhibition of autophagy (12, 13). Taken together, because aberrations in both autophagy and metabolism have been implicated in many cardiac disorders, we questioned whether decorin plays a role in linking these processes with cardiac function.

In this study, we show that decorin is a crucial nutrient sensor *in vivo* that is required for the induction of fasting-mediated cardiac autophagy, a fundamental process that has been shown to be cardioprotective (14, 15). Moreover, we show that $Dcn^{-/-}$ mice differed from WT mice in their cardiac glucose utilization, subsequently resulting in anomalous *O*-GlcNAcylation following nutrient-related stress. We discovered that these differences in autophagy and metabolism altered cardiac function as genetic ablation of decorin preserved ejection fraction following fasting, and this could be reversed by systemic delivery of recombinant decorin. Thus, we present a new role for an extracellular matrix proteoglycan at the epicenter of autophagy and metabolism, which modulates cardiac function. These results contribute to a better understanding of how factors outside the cell are imperative for regulating intracellular processes leading to physiologic consequences. Hence, we propose that these findings will pave the way for other discoveries of outside-in signaling that will enhance our ability to regulate biochemical processes in a manner that will ultimately be useful in a translational setting.

Results

Prolonged fasting cannot transcend the cardiac autophagic defect in $Dcn^{-/-}$ mice

Because our previous work demonstrated the necessity of decorin expression for cardiac autophagy in response to 25-h nutrient deprivation (11) (Fig. S1), we investigated the possibility that prolonged fasting (48 h) could overcome this autophagic impairment in $Dcn^{-/-}$ mice. To this end, we evaluated expression of the lipidated version of microtubule-asso-

This work was supported in part by National Institutes of Health Grants RO1 CA39481, RO1 CA47282, and RO1 CA164462 (to R. V. I.) and National Institutes of Health Training Grant T32 AA07463 (to M. A. G.). The authors declare that they have no conflicts of interest with the contents of this article. The content is solely the responsibility of the authors and does not necessarily represent the official views of the National Institutes of Health.
This article was selected as one of our Editors' Picks.
This article contains Figs. S1–S3, Table S1, Videos S1–S5, and supporting dataset.

[1] To whom correspondence should be addressed. Tel.: 215-955-2208; E-mail: renato.iozzo@jefferson.edu.

[2] The abbreviations used are: RTK, receptor tyrosine kinase; AMPK, adenosine monophosphate kinase; ANOVA, analysis of variance; HBP, hexosamine biosynthetic pathway; IVS, interventricular septal; LVID, left ventricular inner diameter; LVPW, left ventricular posterior wall; *O*-GlcNAcylation, *O*-β-*N*-acetylglycosylation.

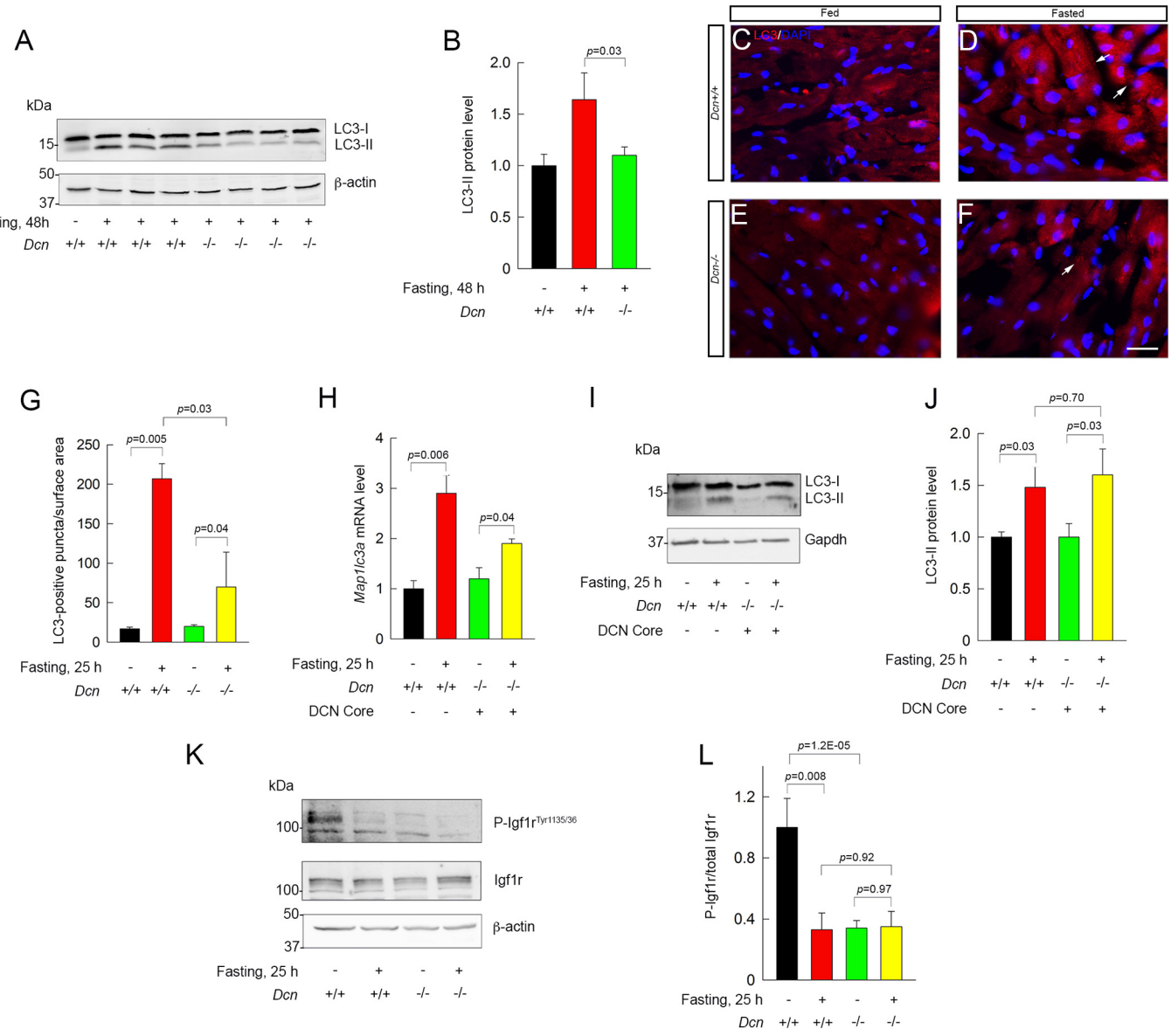

Figure 1. Exogenous decorin treatment, but not prolonged nutrient deprivation, restores fasting-induced autophagy in *Dcn*$^{-/-}$ hearts. *A*, representative Western blotting of LC3 protein levels in WT and *Dcn*$^{-/-}$ hearts following 48 h of fasting. *B*, quantification of (*A*) via densitometric analysis. *C–F*, representative sections of fed and fasted WT and *Dcn*$^{-/-}$ cardiac tissue demonstrating LC3-positive puncta (*red*). Nuclei are stained with DAPI (*blue*). *Arrows* denote the puncta. *Scale bar* ~10 μm. *G*, quantification of LC3-positive puncta seen in *C–F*. *H*, fed and fasted *Map1lc3a* expression levels in WT and decorin-treated *Dcn*$^{-/-}$ hearts. *I*, Western blotting for cardiac LC3 protein levels in fed and fasted WT and decorin-treated *Dcn*$^{-/-}$ mice. *J*, quantification of (*I*). *K*, phosphorylated (Tyr$^{1135/36}$) and total Igf1r expression in WT and *Dcn*$^{-/-}$ hearts in fed and fasted states. *L*, quantification of P-Igf1r/total Igf1r in (*K*). Data represent mean ± S.E. *p* values calculated using Student's *t* test.

ciated light chain protein 3 (LC3-II). Because this lipidated form of LC3 associates with the autophagosomal membrane, quantification of its levels are often used as an accurate approximation of autophagic activity (16). Interestingly, in WT mice, we found that a 48-h fasting resulted in robust conversion of cardiac LC3-I to LC3-II, indicating enhanced autophagic activity, whereas, under the same conditions of nutrient deprivation, LC3-II levels were unchanged in the *Dcn*$^{-/-}$ hearts (Fig. 1*A*). Indeed, 48-h fasted levels of cardiac LC3-II were significantly lower in *Dcn*$^{-/-}$ *vis-à-vis* WT mice (Fig. 1*B*), illustrating that their autophagic capability in response to nutrient deprivation remained impaired even with protracted stimulation of this catabolic pathway. We were curious as to the blunted autophagic response to starvation in the *Dcn*$^{-/-}$heart, and so we delved deeper into the nuances of decorin-mediated cardiac autophagy and found that *Dcn*$^{-/-}$ mice were less sensitive to mTOR inhibition than their WT equivalents. Specifically, we noted lower levels of LC3-II following Torin 1 administration in mice lacking decorin than in WT controls (Fig. S2, *A* and *B*). Moreover, after blocking autophagic flux *in vivo* via chloroquine administration, fasted *Dcn*$^{-/-}$ mice exhibited lower cardiac LC3-II levels than fasted *Dcn*$^{+/+}$ mice, further supporting

the idea that $Dcn^{-/-}$ hearts undergo lower levels of autophagy than $Dcn^{+/+}$ mice (Fig. S2, *C* and *D*). In addition, we examined the levels of another autophagic effector, Beclin 1, and found, as others have (17), that fasting did not change appreciably the levels of Beclin 1 in WT hearts, nor were Beclin 1 levels significantly altered between the two genotypes in either the fed or the fasted state (Fig. S2, *E* and *F*).

We also recognized that our model relied on whole cardiac tissue lysates. To determine which cell types were most affected by lack of decorin, we localized LC3 in cardiac tissue sections primarily to cardiomyocytes. As these cell types make up the majority of the composition of the heart, we concluded that the autophagic differences (quantified here via analysis of LC3-positive puncta) between WT and $Dcn^{-/-}$ hearts were potentially caused by the effects of circulating decorin on these cardiac myocytes (Fig. 1, *C*–*G*). Thus, we hypothesized that decorin acts as an essential nutrient sensor *in vivo* to provoke this catabolic process in cardiac tissue when energy levels are low.

Decorin treatment rescues cardiac autophagy levels in response to nutrient deprivation

Of note, the protein core of decorin interacts with RTKs to modulate intracellular signaling cascades (18–23) whereas the glycosaminoglycan chain is dispensable for most of its biological activity (24, 25). This finding is especially true for its ability to evoke autophagy as we have described previously (7). Therefore, to test our hypothesis that decorin is a nutrient sensor *in vivo*, we treated $Dcn^{-/-}$ mice with recombinant human decorin protein core (10 mg/kg) and then assessed autophagy levels following 25 h of fasting. We first examined expression of the *Map1lc3a* gene encoding LC3, because this gene is inducible by starvation in WT, but not $Dcn^{-/-}$ hearts (11). Remarkably, treatment with exogenous decorin resulted in fasting-mediated induction of this gene in $Dcn^{-/-}$ cardiac tissue, although to levels lower than WT counterparts (Fig. 1*H*). More importantly, decorin treatment caused an increase in LC3-II protein levels in fasted $Dcn^{-/-}$ hearts that was comparable with the levels observed in WT mice following this same period of nutrient deprivation (Fig. 1, *I* and *J*). Therefore, introducing decorin into mice devoid of this proteoglycan rescues the fasting-related autophagic defect in the heart. Interestingly, decorin treatment did not alter levels of LC3-II in the fed state of $Dcn^{-/-}$ hearts compared with fed WT levels (Fig. 1, *I* and *J*). Thus, the pro-autophagic effects of decorin must occur primarily in a nutrient-depleted state, confirming a new role for this small, leucine-rich proteoglycan as a cardiac nutrient sensor to regulate catabolism.

Because decorin is a well-documented pan-RTK inhibitor (5), we surmised that decorin's nutrient-sensing ability must transpire via an outside-in receptor–mediated pathway. Given that the insulin-like growth factor 1 receptor (Igf1r) is a known decorin-binding partner (19, 25, 26) and because Igf1r signaling is vital for both metabolic homeostasis and cardiac function (27), we explored the possibility that $Dcn^{-/-}$ mice display dysregulated signaling through this RTK. Although we found similar expression of total cardiac Igf1r between WT and $Dcn^{-/-}$ mice in both fed and fasted states, we found differential phosphorylation of this receptor at the $Tyr^{1135/36}$ residues (Fig. 1, *K* and *L*). Specifically, there were relatively high levels of Igf1r phosphorylation in the fed state in WT hearts, which were reduced significantly upon 25-h fasting (Fig. 1, *K* and *L*). In contrast, phosphorylated Igf1r in $Dcn^{-/-}$ mice was significantly lower in the fed state and remained low following fasting (Fig. 1, *K* and *L*). This dichotomy in Igf1r phosphorylation status correlated with the relative insensitivity to nutrient-related cues in the absence of decorin. Moreover, combining this aberrant Igf1r phosphorylation with the autophagic deficiency in $Dcn^{-/-}$ hearts suggests potential metabolic irregularities in these mice.

$Dcn^{-/-}$ mice exhibit global metabolism comparable with WT mice

Given these findings, we compared common metabolic parameters in WT and $Dcn^{-/-}$ mice to determine whether systemic differences in metabolism might explain the suppressed autophagy in $Dcn^{-/-}$ hearts. We began by measuring blood glucose in the fed, 25-h fasted, and 48-h fasted states. We chose a consistent time of day (morning) to measure the glucose levels among many mice over multiple experiments to ensure scientifically robust and accurate recordings, especially for the non-fasted animals. Surprisingly, $Dcn^{-/-}$ mice had elevated fed blood glucose levels *vis-à-vis* WT mice (Fig. 2*A*). However, both standard (25 h) and extended (48 h) periods of fasting resulted in similar levels of hypoglycemia in both genotypes (Fig. 2*A*). Despite the higher glucose measurements in $Dcn^{-/-}$ mice in a state of satiety, glucose tolerance was equivalent between WT and $Dcn^{-/-}$ mice (Fig. 2*B*), suggesting intact glucose clearance mechanisms. Moreover, fed and fasted plasma insulin levels were nearly identical between WT and $Dcn^{-/-}$ mice, and both genotypes responded appropriately to fasting by lowering circulating insulin levels (Fig. 2*C*). Looking at other global and cardiac metabolic markers, we again found no major changes between WT and $Dcn^{-/-}$ mice. Specifically, quantification of cardiac glycogen was similar (Fig. 2*D*), as was measurement of circulating and cardiac free fatty acids, both in the fed and fasted state (Fig. 2, *E* and *F*). Hence, WT and $Dcn^{-/-}$ mice demonstrate comparable global metabolic parameters, including glucose clearance and insulin sensitivity with no major perturbations in glycogen turnover or fatty acid metabolism.

High-throughput metabolomics analysis reveals abnormal cardiac glucose utilization in $Dcn^{-/-}$ mice

Next, we considered metabolic differences in WT and $Dcn^{-/-}$ cardiac tissue as they related to nutrient catabolism. To this end, we performed an unbiased, high-throughput MS-based metabolomics study (see also the supporting dataset). Intriguingly, many differences were noted in pathways involving glucose utilization, especially following fasting. We detected a common pattern whereby fasting resulted in increased levels of certain metabolites in WT samples, but this increase was either attenuated or not evident in $Dcn^{-/-}$ hearts. For example, glucose and glucose-6-phosphate were significantly higher in fasted *versus* fed WT hearts (Fig. 3, *A* and *B*). However, this same amount of nutrient deprivation resulted in no significant increase in fasted glucose and a much lower

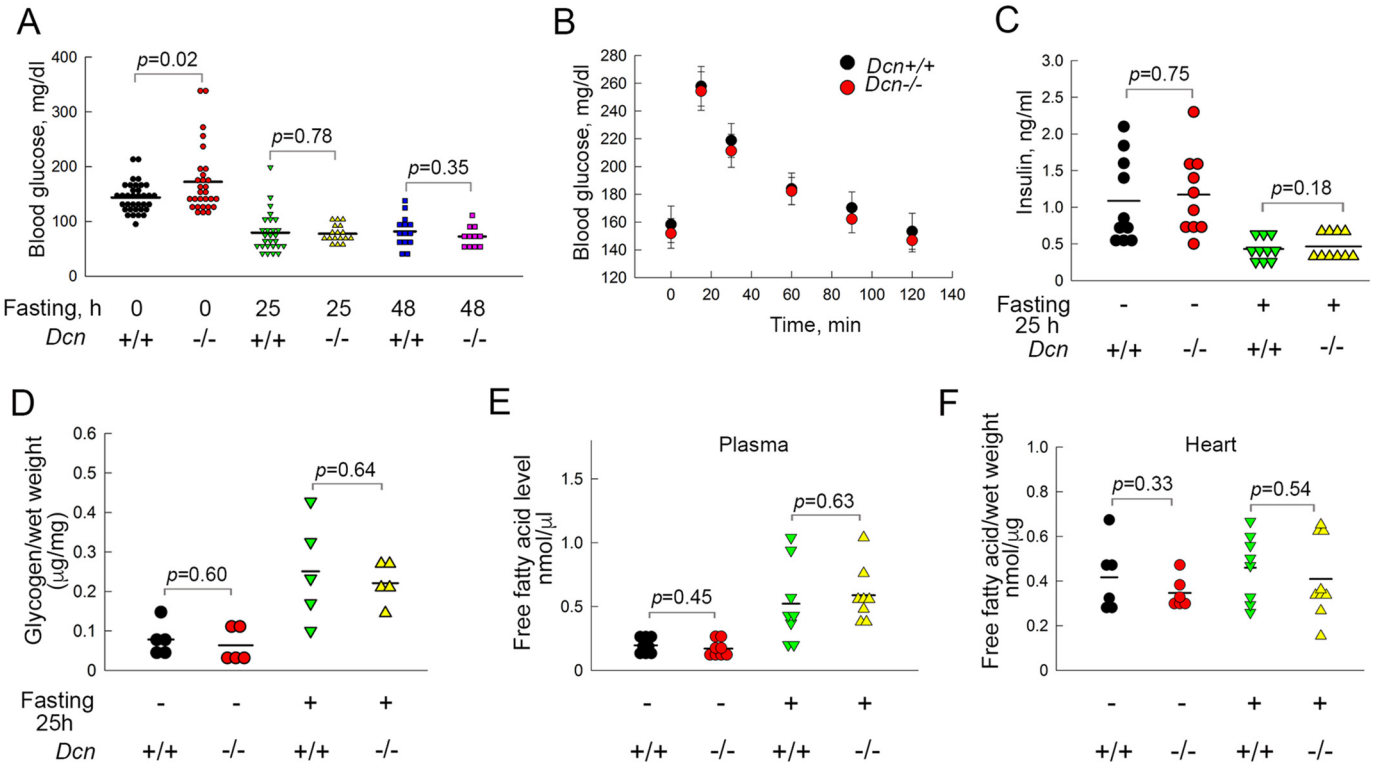

Figure 2. Dcn$^{-/-}$ mice exhibit global metabolism comparable with WT mice. *A*, blood glucose measurements of fed, 25-h fasted, and 48-h fasted WT and *Dcn*$^{-/-}$ mice. *B*, glucose tolerance curves of WT and *Dcn*$^{-/-}$ mice at designated time points. *C*, fed and fasted WT and *Dcn*$^{-/-}$ plasma insulin levels measured via ELISA. *D*, quantification of fed and fasted cardiac glycogen levels. *E* and *F*, fed and fasted free fatty acid levels in WT and *Dcn*$^{-/-}$ mice in plasma (*E*) and cardiac tissue (*F*). Data points represent individual animals. In *B*, data represent mean ± S.E. *p* values calculated using Student's *t* test.

increase in fasted levels of glucose-6-phosphate in *Dcn*$^{-/-}$ cardiac tissue (Fig. 3, *A* and *B*). Indeed, the fasted levels of these metabolites were significantly lower than the amounts measured in WT fasted samples (Fig. 3, *A* and *B*).

Because glucose and glucose-6-phosphate are shuttled through several different pathways, we next examined glycolytic intermediates. We found that 1,6-fructose-bisphosphate followed the aforementioned paradigm, with a blunted response in the fasted state in *Dcn*$^{-/-}$ hearts (Fig. 3*C*). In contrast, the late glycolytic intermediates, 3-phosphoglycerate and its isomer 2-phosphoglycerate, trended toward being higher than the WT levels, particularly in the fasted state (Fig. 3, *D* and *E*). Analysis of the citric acid cycle intermediates aconitate and succinate revealed minimal changes with fasting in WT hearts (Fig. 3, *F* and *G*). In contrast, fasting resulted in decreased levels in *Dcn*$^{-/-}$ cardiac samples (Fig. 3, *F* and *G*). Fasted WT hearts also exhibited increased fumarate, whereas fasting did not alter *Dcn*$^{-/-}$ fumarate levels, although the differences between genotypes in the fasted state were not significant (Fig. 3*H*).

Like glucose, the pentose phosphate pathway intermediates 6-phosphogluconate and sedoheptulose-7-phosphate were increased in fasted WT mice, whereas no significant changes were found with fasting in *Dcn*$^{-/-}$ hearts (Fig. 3, *I* and *J*). Additionally, the UDP sugars UDP-glucose and UDP-galactose were significantly decreased with fasting in WT hearts, but maintained or less significantly decreased with fasting in *Dcn*$^{-/-}$ mice (Fig. 3, *K* and *L*).

Given these differences and given that the heart typically uses fatty acid oxidation under starvation conditions, we focused on glycolytic genes to investigate the possibility that the *Dcn*$^{-/-}$ hearts primarily used glycolysis rather than lipid metabolism during this stressor (Fig. S3, *A–D*). However, although we found differential expression between genotypes of *Pgam2* and *Eno1* following fasting for 25 h (Fig. S3, *C* and *D*), we did not find any significant alterations in protein expression at this time point (Fig. S3, *E–H*). There did appear to be lower levels of Eno1 protein expression in *Dcn*$^{-/-}$ hearts that had undergone 48 h of fasting (Fig. S3, *F* and *H*). However, given that metabolomics data were obtained at the 25 h time point, we did not follow this finding. Thus, we considered an alternate glucose utilization pathway occurring at 25 h to explain these metabolic differences.

Dcn$^{-/-}$ *hearts augment flux through the hexosamine biosynthetic pathway following fasting resulting in increased cardiac O-GlcNAcylation*

Although only 2–5% of glucose enters the HBP, we scrutinized several of its intermediates, as it is a known nutrient and, particularly glucose, sensing pathway. We identified the consistent increase in many metabolites with fasting in WT hearts (fructose, glutamine, glucosamine-6-phosphate), which was attenuated in fasted *Dcn*$^{-/-}$ samples (Fig. 4, *A–C*). Notably, in addition to less pronounced increases with fasting, many of these *Dcn*$^{-/-}$ fasted measurements were significantly lower than the levels in fasted WT tissue (Fig. 4, *A–C*). Of interest, fasting decreased *Dcn*$^{-/-}$ GlcNAc-6-phosphate, whereas its epimer, GlcNAc-1-phosphate, showed only modest differences (Fig. 4, *D* and *E*). Perhaps most noteworthy, uridine diphos-

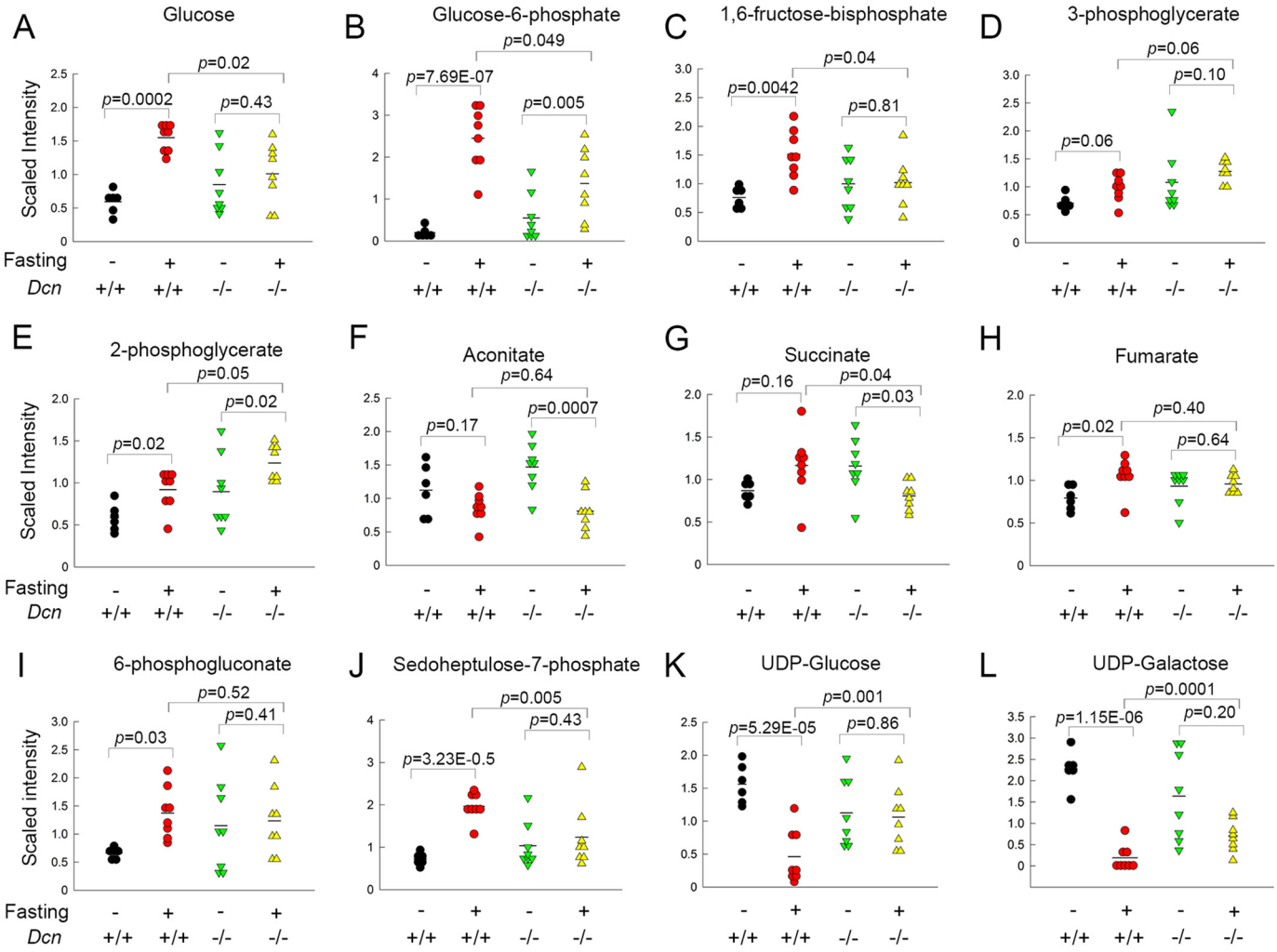

Figure 3. High-throughput metabolomics analysis provides evidence that *Dcn*$^{-/-}$ mice demonstrate anomalous cardiac glucose utilization. Mass spectrometry analysis of fed and 25-h fasted WT and *Dcn*$^{-/-}$ cardiac tissue. *A* and *B*, glucose and glucose-6-phosphate. *C–E*, glycolytic intermediates. *F–H*, citric acid cycle by-products. *I* and *J*, pentose phosphate pathway metabolites. *K* and *L*, UDP sugars. Data points represent individual animals. *p* values calculated via ANOVA contrasts.

phate levels were barely detectable in fasted WT hearts (Fig. 4*F*). However, although a slight decrease was apparent in fasted *Dcn*$^{-/-}$ cardiac tissue, these levels were significantly higher than those seen in the WT samples (Fig. 4*F*).

We must emphasize that this analysis was executed after 25 h of fasting, as the differences in cardiac autophagy levels between WT and *Dcn*$^{-/-}$ mice were unmistakable even with this standard period of nutrient deprivation. Thus, because these measurements were taken at one static time point, these metabolic differences may be because of either increased or decreased flux along these pathways. To gain insight into HBP flux, we analyzed the expression of glutamine fructose-6-phosphate amidotransferase (Gfat), the rate-limiting enzyme of this pathway. We specifically studied Gfat2, as this isoform is most highly expressed in the heart. Remarkably, 25 h of fasting significantly suppressed the expression of this protein in WT hearts (Fig. 4, *G* and *H*). On the contrary, expression of Gfat2 remained constant with fasting in *Dcn*$^{-/-}$ cardiac tissue (Fig. 4, *G* and *H*). Following these findings, we assessed total *O*-GlcNAcylation and found that fasting did not significantly alter this posttranslational modification in WT hearts, although there was a slight trend toward decreased levels. In contrast, fasting caused a nearly significant increase in *O*-GlcNAcylation in *Dcn*$^{-/-}$ cardiac tissue *vis-à-vis* fed equivalents (Fig. 4, *I* and *J*). In fact, fasted cardiac *O*-GlcNAcylation was significantly higher in *Dcn*$^{-/-}$ mice when compared with fasted WT counterparts (Fig. 4*J*). We conclude that *Dcn*$^{-/-}$ mice utilize the HBP in cardiac tissue to a greater extent than WT mice during fasting, resulting in amplified global cardiac protein *O*-GlcNAcylation.

Dcn$^{-/-}$ mice preserve ejection fraction with fasting, which can be reversed by systemic delivery of recombinant decorin

With regard to cardiac function, autophagy holds dual roles as both a protective and pathological mechanism (28). Additionally, proper metabolism is particularly important for maintaining cardiac homeostasis. Because *Dcn*$^{-/-}$ mice exhibit impaired cardiac autophagy and aberrant glucose metabolism, we posited that lack of decorin would cause anomalous cardiac function. Structurally, we found no inherent differences between WT and *Dcn*$^{-/-}$ hearts in terms of diastolic left ventricular internal diameter (LVID), left ventricular posterior wall

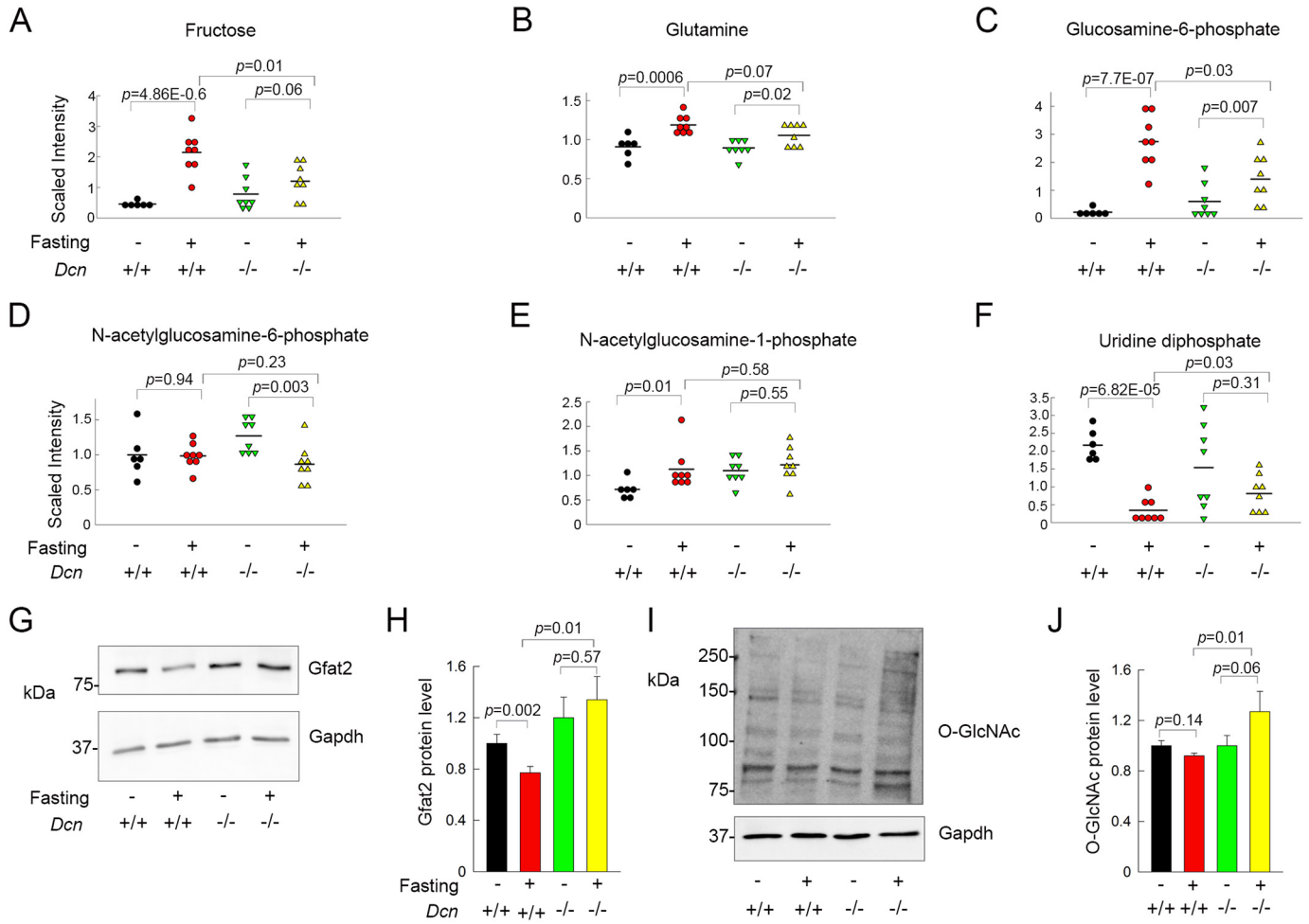

Figure 4. *Dcn*$^{-/-}$ mice augment flux through the hexosamine biosynthetic pathway during fasting, resulting in increased cardiac *O*-GlcNAcylation. *A–F*, MS analysis of hexosamine biosynthetic pathway intermediates in the heart. *G*, representative Western blotting of Gfat2 in fed and 25-h fasted WT and *Dcn*$^{-/-}$ cardiac tissue. *H*, quantification of (*G*). *I*, analysis of global cardiac *O*-GlcNAcylation following 25-h fasting in WT and *Dcn*$^{-/-}$ mice. *J*, quantification of (*I*). Data represent mean ± S.E. *p* values calculated using either ANOVA contrasts (*A–F*) or Student's *t* test (*H* and *J*).

(LVPW) thickness, or interventricular septal (IVS) diameter (Fig. 5, *A–C*). Thus, any functional differences arising between the two genotypes would not be because of structural disparities, but rather because of purely functional alterations. In addition, no changes were noted between genotypes in the following hemodynamic properties: systolic pressure, left ventricular end diastolic pressure, and heart rate (Fig. 5, *D–F*).

Via M-mode echocardiography (Fig. 6, *A–E*), we calculated the ejection fraction for both fed and fasted WT and *Dcn*$^{-/-}$ mice (see also Videos S1–S5). In agreement with published data (29, 30), we found that fasting significantly reduced ejection fraction in WT mice (Fig. 6*F*). Surprisingly, ejection fraction was maintained with fasting in *Dcn*$^{-/-}$ mice (Fig. 6*F*). Most importantly, treatment with decorin protein core reverted the fasted *Dcn*$^{-/-}$ ejection fraction to levels similar to those found in the fasted WT mice (Fig. 6*F*). Hence, we conclude that decorin is a critical nutrient sensor that is imperative for the maintenance of normal cardiac function during low energy states where its absence results in insensitivity to pro-autophagic cues, altered downstream *O*-GlcNAcylation, and inability to properly reduce cardiac output as a means of energy preservation (Fig. 6*G*).

Discussion

The role of the extracellular matrix as a key regulator of intracellular processes and organismal function is becoming increasingly visible (31–40). Decorin is a keystone of this paradigm, where it is implicated in a myriad of signaling pathways to maintain a healthy environment as well as prevent pathology associated with many different diseases, particularly cancer. Our current study provides further evidence that decorin is a significant regulator of critical cellular pathways via receptor-mediated signaling where we have defined a new role for it as a nutrient sensor that modulates cardiac autophagy and metabolism. Taken together, these functions position decorin as a fundamental signaling effector to control cardiac output, especially under nutrient-deficient conditions.

Our recent findings that *Dcn*$^{-/-}$ mice exhibit reduced cardiac autophagy even with prolonged nutrient deprivation and the ability of exogenous decorin to provoke an autophagic response in these same mice provide a new model for outside-in signaling. Specifically, the fact that decorin only rescues autophagic levels *in vivo* following fasting suggests that it is not so much the mere presence of decorin, but rather its localiza-

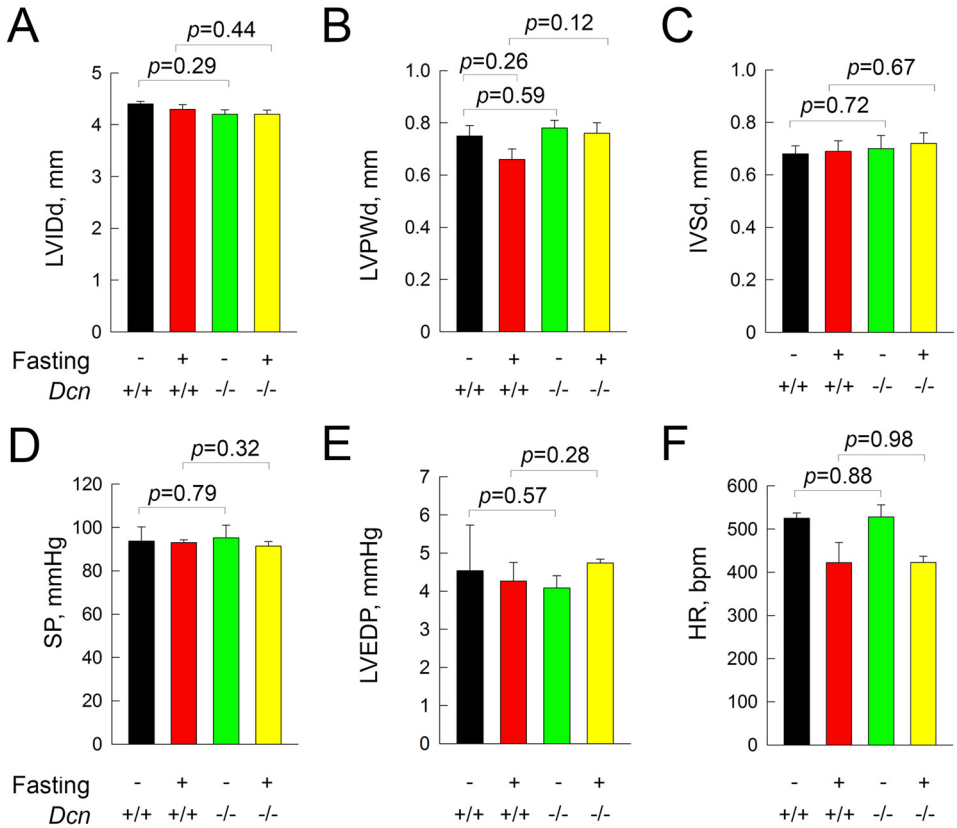

Figure 5. There are no apparent structural disparities between WT and *Dcn*$^{-/-}$ hearts. *A–C*, echocardiography analysis of (*A*) left ventricular inner diameter (*LVIDd*), (*B*) left ventricular posterior wall thickness (*LVPWd*), and (*C*) interventricular septal diameter (*IVSd*) in diastole. *D–F*, hemodynamic analysis of (*D*) systolic pressure (*SP*), (*E*) left ventricular end diastolic pressure (*LVEDP*), (*F*) heart rate (*HR*). Data represent mean ± S.E. *p* values calculated using Student's *t* test.

tion and/or binding partners during nutrient deprivation that promote autophagy. Our investigation of Igf1r signaling supports this idea in that in both the fed and fasted states of *Dcn*$^{-/-}$ hearts, there is minimal phosphorylation of this receptor, signifying insensitivity to extracellular cues in the absence of decorin. As decorin binds and signals through Igf1r via its protein core, it is likely that this receptor–ligand interaction is responsible for these findings. Alternatively, as decorin binds several growth factors, including Igf-1 (1, 19), this deviant signaling could also be because of impaired presentation of the growth factor to its receptor. However, given that recombinant decorin core was able to restore normal autophagy in response to fasting, it is more likely that the former rather than the latter is at play. Further study must be undertaken in this avenue to parse out the exact role that decorin plays in these processes with a focused emphasis on which binding partners are members of this intricate assembly.

Given the differential phosphorylation of cardiac Igf1r in the absence of decorin, we were somewhat surprised to find few alterations in common metabolism markers between WT and *Dcn*$^{-/-}$ mice. Although the *Dcn*$^{-/-}$ mice display elevated fed blood glucose levels, they are not glucose intolerant or insulin resistant, suggesting they are not overtly diabetic or even prediabetic. Intriguingly, anecdotal observations from our lab note that some, but not all, *Dcn*$^{-/-}$ mice demonstrate increased abdominal adiposity when compared with WT mice, especially as they age. Interestingly, proteomic analysis of obese patients illustrates an accumulation of decorin in adipose tissue (41). However, these studies were purely observational and no real function for increased decorin expression in adipose tissue has been elucidated as of yet. Therefore, we believe that decorin is important for global metabolic homeostasis, although the exact mechanism is still to be determined.

Despite only subtle global metabolic differences, we were encouraged to find conspicuous cardiac metabolic disparities *vis-à-vis* WT mice, particularly prominent in the HBP. Importantly, an independent metabolomics study similarly reported altered cardiac metabolism in *Dcn*$^{-/-}$ mice (42), although in the context of atrial fibrillation and not starvation. These metabolic aberrations may help explain the *Dcn*$^{-/-}$ autophagic defect, as recent evidence supports the hypothesis that increased *O*-GlcNAcylation inhibits autophagy. In a diabetic model, pharmacologically increasing *O*-GlcNAcylation blunts autophagic signaling specifically in cardiac tissue (13). Other studies provide a role for *O*-GlcNAcylation as a means to prevent autophagosome maturation by interfering with SNARE proteins (43). In addition, Torin 1, a potent pro-autophagic compound, inhibits *O*-GlcNAc transferase, the enzyme that catalyzes *O*-GlcNAcylation, while simultaneously inducing the antithetic *O*-GlcNAcase, which removes these posttranslational modifications (44). Finally, loss of expression of Gfat, the HBP rate-limiting enzyme, enhances autophagy as measured by increases in LC3-positive puncta (43). Moreover, acute increases in *O*-GlcNAcylation can act as a stress response.

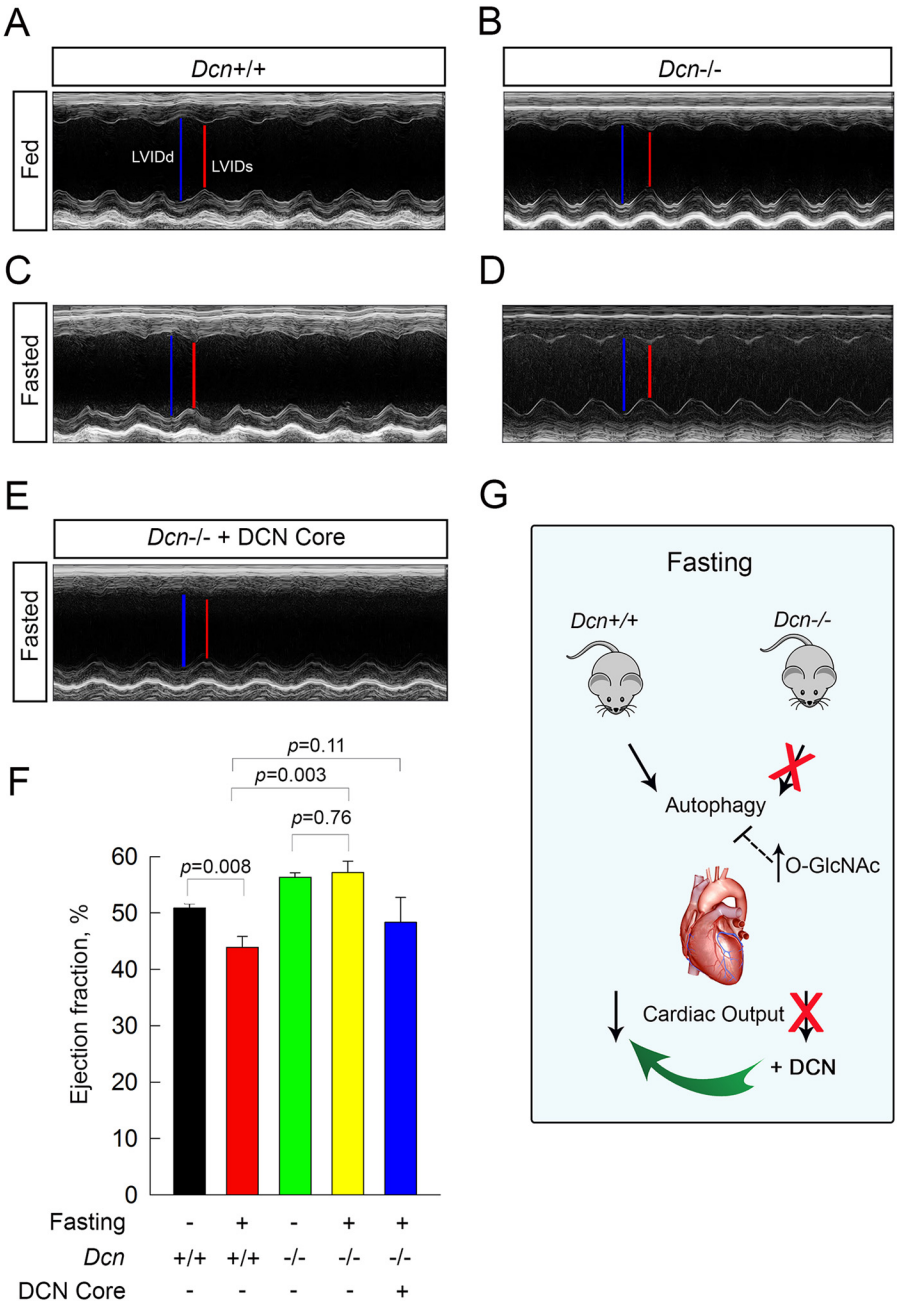

Figure 6. Dcn$^{-/-}$ mice preserve ejection fraction following fasting, which can be reverted to WT levels upon decorin treatment. *A–E*, representative echocardiograms in fed and fasted WT and *Dcn*$^{-/-}$ hearts. *Blue lines* represent LVID in diastole and *red lines* represent LVID in systole (see Videos S1–S5). *F*, quantification of calculated ejection fraction as seen in (*A–E*). *G*, schematic demonstrating the finding that decorin is necessary to invoke autophagy and reduce ejection fraction during starvation. Data represent mean ± S.E. *p* values calculated using Student's *t* test.

Thus, the higher baseline levels of glucose in the fed state and increased *O*-GlcNAcylation seen in fasted *Dcn*$^{-/-}$ cardiac tissue indicate that this altered sugar usage could be an unorthodox mechanism in response to nutrient-related stress, which may directly inhibit an autophagic response. Perhaps even more interestingly, our earlier work shows that decorin is upregulated in the heart during periods of fasting (11). Hence, it is possible that, during fasting, the WT heart moves toward a biosynthetic state resulting in the diversion of UDP-GlcNAc into proteoglycan synthesis, whereas in the absence of decorin, the cardiac extracellular matrix improperly shunts this moiety toward global *O*-GlcNAcylation.

Our findings regarding cardiac functional differences were quite remarkable. Just as we found, other studies report that fasting reduces ejection fraction (29, 30). Although autophagy may be the main mechanism to recycle nutrients to sustain cardiac homeostasis in WT hearts, the reduction in ejection fraction may be an additional fail-safe to further support cardiomyocyte survival when food availability is low. In contrast, the ability for *Dcn*$^{-/-}$ mice to maintain cardiac output with fasting aligns with our previous observation that these mice do not detect differences in nutrient status. Interestingly, data from a hemorrhagic model study show that glucosamine infusion increases cardiac *O*-GlcNAcylation and cardiac output

(45). Therefore, the increased *O*-GlcNAcylation during fasting may be the cause of sustained ejection fraction in the $Dcn^{-/-}$ mice. Of note, although this preservation of cardiac function with fasting appears at first glance to be advantageous, it may also be problematic as continual normal cardiac function in the context of reduced nutrient supply may lead to adverse events, such as myocardial infarction, especially if nutrient deprivation is combined with another stressor, such as extreme exercise or sepsis.

Additionally, we must comment that *O*-GlcNAcylation enhances the expression of hyaluronan synthase 2 (HAS2), a critical mediator of hyaluronan synthesis (46, 47). Although our study did not address this consequence of increased *O*-GlcNAcylation, it is possible that there exists aberrant hyaluronan expression and signaling in these $Dcn^{-/-}$ hearts, particularly during fasting. Additionally, especially under periods of prolonged nutrient deprivation, there may be a complex interplay between the adenosine monophosphate kinase (AMPK)–signaling axis and HAS2 regulation, as AMPK activation has been shown to reduce HAS2 activity (48). Further investigation is warranted to identify a connection among the autophagic defect including AMPK signaling, the preserved ejection fraction, and the hyaluronan signaling pathway in the absence of decorin.

Taken together, these new findings illuminate decorin as a fundamental extracellular signaling molecule that simultaneously regulates cardiac autophagy, metabolism, and function during nutrient deprivation. Given this information, decorin may prove to be important as both a prognostic and diagnostic marker for heart disease and could also be an effective therapeutic option to regulate cardiac metabolism in the setting of obesity or diabetes. Furthermore, we believe that future investigation will yield many more extracellular proteoglycans and other associated matrix members as key players in this elaborate network. Thus, we provide an additional meaningful function to decorin's already extensive repertoire and further underscore the importance of the extracellular matrix for normal cell signaling.

Experimental procedures

Chemicals and antibodies

Antibodies were purchased as follows: Actb (Abcam, ab8227), Beclin 1 (Cell Signaling Technology, 3738), Eno1 (Abcam, ab49343), GAPDH (Cell Signaling Technology, 2118), Gfat2 (Abcam, ab155926), total Igf1r (Santa Cruz Biotechnology, sc-713), P-Igf1r$^{Tyr1135/36}$ (Cell Signaling Technology, 3024), LC3 (Sigma, L7543), *O*-GlcNAc CTD.110.6 (Cell Signaling Technology, 9875), and phosphoglycerate mutase 2 (Abcam, ab187147). All antibodies were used at a 1:1000 dilution for Western blotting and 1:500 for immunofluorescence except Actb and GAPDH, which were used at 1:10,000. Decorin was purified as described previously (49). Goat anti-rabbit and anti-mouse secondary antibodies conjugated with HRP (12–348, 12–349) were purchased from EMD Millipore and used at 1:4000 dilution. Torin 1 (42–471-0) was purchased from Tocris.

Animal experiments

C57BL/6 mice were purchased from The Jackson Laboratory. Global $Dcn^{-/-}$ mice were generated as described previously (50). Animal experiments were performed as per the Guide for Care and Use of Laboratory Animals and the Institutional Animal Care and Use Committee of Thomas Jefferson University. Mice were of both male and female sex ranging from 2–4 months of age. Fasting experiments involved withholding food for 25 or 48 h, but water was allowed *ad libitum*. Equal numbers of male and female mice were used for each experiment. After animals were euthanized, organs were removed and immediately snap-frozen in liquid N_2. For rescue experiments, mice were injected intraperitoneally with 10 mg/kg of purified human decorin protein core every other day for 1 week before fasting and sacrifice. For *in vivo* flux experiments, mice were fasted for 25 h and 6 h before sacrifice were injected intraperitoneally with 100 mg/kg chloroquine. Torin 1 was administered via intraperitoneal injection at a concentration of 5 mg/kg.

Echocardiography

Cardiac function was assessed via echocardiography, which was performed with the VisualSonics VeVo 2100 imaging system in animals anesthetized with 1.5% v/v isoflurane. The internal diameter of the left ventricle was measured in the short-axis view from M-mode recordings in end diastole and end systole. Hemodynamic measurements were obtained via carotid artery catheterization.

Metabolomics analysis

Cardiac tissue from WT and $Dcn^{-/-}$ mice that had been either fed *ad libitum* or subjected to 25 h fasting were analyzed by Metabolon, Inc. using a predetermined dataset of 554 compounds. Cardiac metabolites were measured with a high-resolution accurate mass platform of ultrahigh performance LC/MS and GC/MS. All analyses included acquisition of raw data, peak identification, and comparison with several quality control samples. The complete dataset can be found as supporting information.

Measurement of metabolic parameters

Blood glucose was measured using a standard blood glucometer. Insulin levels were assessed using an ELISA specific for mouse insulin (Crystal Chem, 90080). Glycogen and free fatty acid levels were measured using colorimetric assays as per the manufacturer's directions (Sigma, MAK016 and MAK044). For glucose tolerance tests, mice were fasted for 4 h followed by oral gavage of 2g/kg 25% glucose solution. Blood glucose was measured via glucometer at 0, 15, 30, 60, 90, and 120 min.

Western blotting and immunofluorescence analysis

Tissue samples were lysed in T-Per Reagent with EDTA and protease inhibitor (Life Technologies, 78510). Samples were separated by SDS-PAGE and transferred to nitrocellulose where specific antibodies were used to visualize the proteins. Immunofluorescence was performed as described previously (51, 52). In brief, cardiac sections were fixed with paraformal-

dehyde and stained with an LC3-specific antibody. Nuclei were visualized with DAPI. Quantification of LC3 puncta was performed using a macro specific for ImageJ software that was designed by Ruben Dagda (University of Nevada School of Medicine) (53, 54).

Quantitative real-time PCR analysis

One mm^3 of tissue was lysed in 750 μl of TRIzol® reagent (Life Technologies, 15596–026). RNA was isolated using a standard RNA isolation kit (Zymo Research, R2052). One μg of RNA was annealed with oligo(dT) primers (Life Technologies, 18418–012), and cDNA was synthesized using SuperScript Reverse Transcriptase II (Life Technologies, 18064–022) according to the manufacturer's directions. The target genes (primer sequences can be found in Table S1) and housekeeping gene (*Actb*) were amplified in independent reactions using the Brilliant SYBR Green Master Mix II (Agilent Technologies, 600828). Samples were run in duplicate on a LightCycler480-II (Roche Applied Science) and the cycle number (C_t) was obtained for each reaction. The -fold change determinations were made utilizing the comparative C_t method for gene expression analysis.

Quantification and statistical analysis

Experiments were repeated three or more times and all data are expressed as means ± S.E. Paired and unpaired two-tailed Student's *t*-tests were used to analyze significance using the SigmaStat program. $p < 0.05$ was considered statistically significant. For the metabolomics analysis, following log transformation and imputation of missing values, if any, with the minimum observed value for each compound, analysis of variance (ANOVA) contrasts were used to identify biochemicals that differed significantly between experimental groups. A summary of the numbers of biochemicals that achieved statistical significance ($p \leq 0.05$), as well as those approaching significance ($0.05 < p < 0.10$) were noted (see supporting dataset). Analysis by two-way ANOVA identified biochemicals exhibiting significant interaction and main effects for experimental parameters of genotype and feed status.

Author contributions—M. A. G., U. R., J. B. H., and R. V. I. conceptualization; M. A. G., E. L. S., and R. V. I. data curation; M. A. G., E. L. S., U. R., J. B. H., and R. V. I. formal analysis; M. A. G. and R. V. I. validation; M. A. G. and R. V. I. investigation; M. A. G. and R. V. I. visualization; M. A. G., E. L. S., U. R., J. B. H., and R. V. I. methodology; M. A. G. and R. V. I. writing-original draft; M. A. G., E. L. S., U. R., J. B. H., and R. V. I. writing-review and editing; R. V. I. resources; R. V. I. software; R. V. I. supervision; R. V. I. funding acquisition; R. V. I. project administration.

Acknowledgments—Thank you to R. T. Owens for providing the recombinant decorin, and Nadan Wang of the Small Animal Physiology Core of Thomas Jefferson University for technical expertise and guidance of the cardiac functional studies.

References

1. Gubbiotti, M. A., Vallet, S. D., Ricard-Blum, S., and Iozzo, R. V. (2016) Decorin interacting network: A comprehensive analysis of decorin-binding partners and their versatile functions. *Matrix Biol.* **55,** 7–21 CrossRef Medline
2. Iozzo, R. V., and Schaefer, L. (2015) Proteoglycan form and function: A comprehensive nomenclature of proteoglycans. *Matrix Biol.* **42,** 11–55 CrossRef Medline
3. Iozzo, R. V., Goldoni, S., Berendsen, A. D., and Young, M. F. (2011) Small leucine-rich proteoglycans. in *Extracellular Matrix: An Overview* (Mecham, R. P., ed) pp. 197–231, Springer, Berlin, Germany CrossRef
4. Neill, T., Schaefer, L., and Iozzo, R. V. (2015) Oncosuppressive role for decorin. *Mol. Cell. Oncol.* **2,** e975645 CrossRef Medline
5. Neill, T., Schaefer, L., and Iozzo, R. V. (2015) Decoding the matrix: Instructive roles of proteoglycan receptors. *Biochemistry* **54,** 4583–4598 CrossRef Medline
6. Neill, T., Schaefer, L., and Iozzo, R. V. (2012) Decorin, a guardian from the matrix. *Am. J. Pathol.* **181,** 380–387 CrossRef Medline
7. Buraschi, S., Neill, T., Goyal, A., Poluzzi, C., Smythies, J., Owens, R. T., Schaefer, L., Torres, A., and Iozzo, R. V. (2013) Decorin causes autophagy in endothelial cells via Peg3. *Proc. Natl. Acad. Sci. U.S.A.* **110,** E2582–E2591 CrossRef Medline
8. Gubbiotti, M. A., and Iozzo, R. V. (2015) Proteoglycans regulate autophagy via outside-in signaling: An emerging new concept. *Matrix Biol.* **48,** 6–13 CrossRef Medline
9. Yao, T., Zhang, C. G., Gong, M. T., Zhang, M., Wang, L., and Ding, W. (2016) Decorin-mediated inhibition of the migration of U87MG glioma cells involves activation of autophagy and suppression of TGF-β signaling. *FEBS Open Bio.* **6,** 707–719 CrossRef Medline
10. Neill, T., Torres, A., Buraschi, S., Owens, R. T., Hoek, J. B., Baffa, R., and Iozzo, R. V. (2014) Decorin induces mitophagy in breast carcinoma cells via peroxisome proliferator-activated receptor γ coactivator-1α (PGC-1α) and mitostatin. *J. Biol. Chem.* **289,** 4952–4968 CrossRef Medline
11. Gubbiotti, M. A., Neill, T., Frey, H., Schaefer, L., and Iozzo, R. V. (2015) Decorin is an autophagy-inducible proteoglycan and is required for proper *in vivo* autophagy. *Matrix Biol.* **48,** 14–25 CrossRef Medline
12. Bond, M. R., and Hanover, J. A. (2015) A little sugar goes a long way: The cell biology of *O*-GlcNAc. *J. Cell Biol.* **208,** 869–880 CrossRef Medline
13. Marsh, S. A., Powell, P. C., Dell'italia, L. J., and Chatham, J. C. (2013) Cardiac *O*-GlcNAcylation blunts autophagic signaling in the diabetic heart. *Life Sci.* **92,** 648–656 CrossRef Medline
14. Jahania, S. M., Sengstock, D., Vaitkevicius, P., Andres, A., Ito, B. R., Gottlieb, R. A., and Mentzer, R. M., Jr. (2013) Activation of the homeostatic intracellular repair response during cardiac surgery. *J. Am. Coll. Surg.* **216,** 719–726; discussion 726–729 CrossRef Medline
15. Matsui, Y., Takagi, H., Qu, X., Abdellatif, M., Sakoda, H., Asano, T., Levine, B., and Sadoshima, J. (2007) Distinct roles of autophagy in the heart during ischemia and reperfusion: Roles of AMP-activated protein kinase and Beclin 1 in mediating autophagy. *Circ. Res.* **100,** 914–922 CrossRef Medline
16. Mizushima, N., Yoshimori, T., and Levine, B. (2010) Methods in mammalian autophagy research. *Cell* **140,** 313–326 CrossRef Medline
17. Zhu, H., Tannous, P., Johnstone, J. L., Kong, Y., Shelton, J. M., Richardson, J. A., Le, V., Levine, B., Rothermel, B. A., and Hill, J. A. (2007) Cardiac autophagy is a maladaptive response to hemodynamic stress. *J. Clin. Invest.* **117,** 1782–1793 CrossRef Medline
18. Neill, T., Painter, H., Buraschi, S., Owens, R. T., Lisanti, M. P., Schaefer, L., and Iozzo, R. V. (2012) Decorin antagonizes the angiogenic network. Concurrent inhibition of Met, hypoxia inducible factor-1α and vascular endothelial growth factor A and induction of thrombospondin-1 and TIMP3. *J. Biol. Chem.* **287,** 5492–5506 CrossRef Medline
19. Morrione, A., Neill, T., and Iozzo, R. V. (2013) Dichotomy of decorin activity on the insulin-like growth factor-I system. *FEBS J.* **280,** 2138–2149 CrossRef Medline
20. Moscatello, D. K., Santra, M., Mann, D. M., McQuillan, D. J., Wong, A. J., and Iozzo, R. V. (1998) Decorin suppresses tumor cell growth by activating the epidermal growth factor receptor. *J. Clin. Invest.* **101,** 406–412 CrossRef Medline
21. Iozzo, R. V., Moscatello, D. K., McQuillan, D. J., and Eichstetter, I. (1999) Decorin is a biological ligand for the epidermal growth factor receptor. *J. Biol. Chem.* **274,** 4489–4492 CrossRef Medline

22. Goldoni, S., Humphries, A., Nyström, A., Sattar, S., Owens, R. T., McQuillan, D. J., Ireton, K., and Iozzo, R. V. (2009) Decorin is a novel antagonistic ligand of the Met receptor. *J. Cell Biol.* **185,** 743–754 CrossRef Medline
23. Buraschi, S., Pal, N., Tyler-Rubinstein, N., Owens, R. T., Neill, T., and Iozzo, R. V. (2010) Decorin antagonizes Met receptor activity and down-regulates β-catenin and Myc levels. *J. Biol. Chem.* **285,** 42075–42085 CrossRef Medline
24. Buraschi, S., Neill, T., Owens, R. T., Iniguez, L. A., Purkins, G., Vadigepalli, R., Evans, B., Schaefer, L., Peiper, S. C., Wang, Z. X., and Iozzo, R. V. (2012) Decorin protein core affects the global gene expression profile of the tumor microenvironment in a triple-negative orthotopic breast carcinoma xenograft model. *PLoS One* **7,** e45559 CrossRef Medline
25. Schönherr, E., Sunderkötter, C., Iozzo, R. V., and Schaefer, L. (2005) Decorin, a novel player in the insulin-like growth factor system. *J. Biol. Chem.* **280,** 15767–15772 CrossRef Medline
26. Iozzo, R. V., Buraschi, S., Genua, M., Xu, S.-Q., Solomides, C. C., Peiper, S. C., Gomella, L. G., Owens, R. C., and Morrione, A. (2011) Decorin antagonizes IGF receptor I (IGF-IR) function by interfering with IGF-IR activity and attenuating downstream signaling. *J. Biol. Chem.* **286,** 34712–34721 CrossRef Medline
27. Troncoso, R., Ibarra, C., Vicencio, J. M., Jaimovich, E., and Lavandero, S. (2014) New insights into IGF-1 signaling in the heart. *Trends Endocrinol. Metab.* **25,** 128–137 CrossRef Medline
28. Lavandero, S., Chiong, M., Rothermel, B. A., and Hill, J. A. (2015) Autophagy in cardiovascular biology. *J. Clin. Invest.* **125,** 55–64 CrossRef Medline
29. Baskin, K. K., and Taegtmeyer, H. (2011) AMP-activated protein kinase regulates E3 ligases in rodent heart. *Circ. Res.* **109,** 1153–1161 CrossRef Medline
30. Suzuki, J., Ueno, M., Uno, M., Hirose, Y., Zenimaru, Y., Takahashi, S., Osuga, J., Ishibashi, S., Takahashi, M., Hirose, M., Yamada, M., Kraemer, F. B., and Miyamori, I. (2009) Effects of hormone-sensitive lipase disruption on cardiac energy metabolism in response to fasting and refeeding. *Am. J. Physiol. Endocrinol. Metab.* **297,** E1115–E1124 CrossRef Medline
31. Ghadiali, R. S., Guimond, S. E., Turnbull, J. E., and Pisconti, A. (2017) Dynamic changes in heparan sulfate during muscle differentiation and ageing regulate myoblast cell fate and FGF2 signalling. *Matrix Biol.* **59,** 54–68 CrossRef Medline
32. Naba, A., Clauser, K. R., Ding, H., Whittaker, C. A., Carr, S. A., and Hynes, R. O. (2016) The extracellular matrix: Tools and insights for the "omics" era. *Matrix Biol.* **49,** 10–24 CrossRef Medline
33. Randles, M. J., Humphries, M. J., and Lennon, R. (2017) Proteomic definitions of basement membrane composition in health and disease. *Matrix Biol.* **57–58,** 12–28 CrossRef Medline
34. Pozzi, A., Yurchenco, P. D., and Iozzo, R. V. (2017) The nature and biology of basement membranes. *Matrix Biol.* **57–58,** 1–11 CrossRef Medline
35. Gubbiotti, M. A., Neill, T., and Iozzo, R. V. (2017) A current view of perlecan in physiology and pathology: A mosaic of functions. *Matrix Biol.* **57–58,** 285–298 CrossRef Medline
36. Andreuzzi, E., Colladel, R., Pellicani, R., Tarticchio, G., Cannizzaro, R., Spessotto, P., Bussolati, B., Brossa, A., De Paoli, P., Canzonieri, V., Iozzo, R. V., Colombatti, A., and Mongiat, M. (2017) The angiostatic molecule Multimerin 2 is processed by MMP-9 to allow sprouting angiogenesis. *Matrix Biol.* **64,** 40–53 CrossRef Medline
37. Karousou, E., Misra, S., Ghatak, S., Dobra, K., Götte, M., Vigetti, D., Passi, A., Karamanos, N. K., and Skandalis, S. S. (2017) Roles and targeting of the HAS/hyaluronan/CD44 molecular system in cancer. *Matrix Biol.* **59,** 3–22 CrossRef Medline
38. Uitto, J., Has, C., Vahidnezhad, H., Youssefian, L., and Bruckner-Tuderman, L. (2017) Molecular pathology of the basement membrane zone in heritable blistering diseases: The paradigm of epidermolysis bullosa. *Matrix Biol.* **57–58,** 76–85 CrossRef Medline
39. Young, M. F. (2016) Skeletal biology: Where matrix meets mineral. *Matrix Biol.* **52–54,** 1–6 CrossRef Medline
40. Prockop, D. J. (2016) Inflammation, fibrosis, and modulation of the process by mesenchymal stem/stromal cells. *Matrix Biol.* **51,** 7–13 CrossRef Medline
41. Bolton, K., Segal, D., McMillan, J., Jowett, J., Heilbronn, L., Abberton, K., Zimmet, P., Chisholm, D., Collier, G., and Walder, K. (2008) Decorin is a secreted protein associated with obesity and type 2 diabetes. *Int. J. Obes.* **32,** 1113–1121 CrossRef Medline
42. Barallobre-Barreiro, J., Gupta, S. K., Zoccarato, A., Kitazume-Taneike, R., Fava, M., Yin, X., Werner, T., Hirt, M. N., Zampetaki, A., Viviano, A., Chong, M., Bern, M., Kourliouros, A., Domenech, N., Willeit, P., *et al.* (2016) Glycoproteomics reveals decorin peptides with anti-myostatin activity in human atrial fibrillation. *Circulation* **134,** 817–832 CrossRef Medline
43. Guo, B., Liang, Q., Li, L., Hu, Z., Wu, F., Zhang, P., Ma, Y., Zhao, B., Kovács, A. L., Zhang, Z., Feng, D., Chen, S., and Zhang, H. (2014) *O*-GlcNAc-modification of SNAP-29 regulates autophagosome maturation. *Nat. Cell Biol.* **16,** 1215–1226 CrossRef Medline
44. Park, S., Pak, J., Jang, I., and Cho, J. W. (2014) Inhibition of mTOR affects protein stability of OGT. *Biochem. Biophys. Res. Commun.* **453,** 208–212 CrossRef Medline
45. Yang, S., Zou, L. Y., Bounelis, P., Chaudry, I., Chatham, J. C., and Marchase, R. B. (2006) Glucosamine administration during resuscitation improves organ function after trauma hemorrhage. *Shock* **25,** 600–607 CrossRef Medline
46. Vigetti, D., Deleonibus, S., Moretto, P., Bowen, T., Fischer, J. W., Grandoch, M., Oberhuber, A., Love, D. C., Hanover, J. A., Cinquetti, R., Karousou, E., Viola, M., D'Angelo, M. L., Hascall, V. C., De Luca, G., and Passi, A. (2014) Natural antisense transcript for hyaluronan synthase 2 (HAS2-AS1) induces transcription of HAS2 via protein *O*-GlcNAcylation. *J. Biol. Chem.* **289,** 28816–28826 CrossRef Medline
47. Vigetti, D., Deleonibus, S., Moretto, P., Karousou, E., Viola, M., Bartolini, B., Hascall, V. C., Tammi, M., De Luca, G., and Passi, A. (2012) Role of UDP-*N*-acetylglucosamine (GlcNAc) and *O*-GlcNAcylation of hyaluronan synthase 2 in the control of chondroitin sulfate and hyaluronan synthesis. *J. Biol. Chem.* **287,** 35544–35555 CrossRef Medline
48. Vigetti, D., Clerici, M., Deleonibus, S., Karousou, E., Viola, M., Moretto, P., Heldin, P., Hascall, V. C., De Luca, G., and Passi, A. (2011) Hyaluronan synthesis is inhibited by adenosine monophosphate-activated protein kinase through the regulation of HAS2 activity in human aortic smooth muscle cells. *J. Biol. Chem.* **286,** 7917–7924 CrossRef Medline
49. Reed, C. C., Waterhouse, A., Kirby, S., Kay, P., Owens, R. T., McQuillan, D. J., and Iozzo, R. V. (2005) Decorin prevents metastatic spreading of breast cancer. *Oncogene* **24,** 1104–1110 CrossRef Medline
50. Danielson, K. G., Baribault, H., Holmes, D. F., Graham, H., Kadler, K. E., and Iozzo, R. V. (1997) Targeted disruption of decorin leads to abnormal collagen fibril morphology and skin fragility. *J. Cell Biol.* **136,** 729–743 CrossRef Medline
51. Ryynänen, M., Ryynänen, J., Sollberg, S., Iozzo, R. V., Knowlton, R. G., and Uitto, J. (1992) Genetic linkage of type VII collagen (COL7A1) to dominant dystrophic epidermolysis bullosa in families with abnormal anchoring fibrils. *J. Clin. Invest.* **89,** 974–980 CrossRef Medline
52. Rudnicka, L., Varga, J., Christiano, A. M., Iozzo, R. V., Jimenez, S. A., and Uitto, J. (1994) Elevated expression of type VII collagen in the skin of patients with systemic sclerosis. *J. Clin. Invest.* **93,** 1709–1715 CrossRef Medline
53. Chu, C. T., Plowey, E. D., Dagda, R. K., Hickey, R. W., Cherra, S. J., 3rd, and Clark, R. S. (2009) Autophagy in neurite injury and neurodegeneration: *In vitro* and *in vivo* models. *Methods Enzymol.* **453,** 217–249 CrossRef Medline
54. Dagda, R. K., Zhu, J., Kulich, S. M., and Chu, C. T. (2008) Mitochondrially localized ERK2 regulates mitophagy and autophagic cell stress: implications for Parkinson's disease. *Autophagy* **4,** 770–782 CrossRef Medline

Metabolic reprogramming of murine cardiomyocytes during autophagy requires the extracellular nutrient sensor decorin

Maria A. Gubbiotti, Erin Seifert, Ulrich Rodeck, Jan B. Hoek and Renato V. Iozzo

J. Biol. Chem. 2018, 293:16940-16950.
doi: 10.1074/jbc.RA118.004563 originally published online July 26, 2018